frontiers in Nanotechnology

ORIGINAL RESEARCH
published: 08 September 2021
doi: 10.3389/fnano.2021.689718

Characterization of MXene as a Cancer Photothermal Agent Under Physiological Conditions

Samar Shurbaji[1], Nimshitha P. Abdul Manaph[2], Samia M. Ltaief[2], Abeer R. Al-Shammari[2], Ahmed Elzatahry[3] and Huseyin C. Yalcin[1,4]**

[1]Biomedical Research Center, Qatar University, Doha, Qatar, [2]Neurological Disorders Research Center, Qatar Biomedical Research Institute, Hamad Bin Khalifa University, Qatar Foundation, Doha, Qatar, [3]Materials Science and Technology Department, College of Arts and Sciences, Qatar University, Doha, Qatar, [4]Department of Biomedical Sciences, College of Health Science-QU Health, Qatar University, Doha, Qatar*

A growing interest has recently emerged in the use of nanomaterials in medical applications. Nanomaterials, such as MXene, have unique properties due to their 2D ultra-thin structure, which is potentially useful in cancer photothermal therapy. To be most effective, photothermal agents need to be internalized by the cancer cells. In this study, MXene was fabricated using chemical reactions and tested as a photothermal agent on MDA-231 breast cancer cells under static and physiological conditions. Fluid shear stress (~0.1 Dyn/cm^2) was applied using a perfusion system to mimic the physiological tumor microenvironment. The uptake of MXene was analyzed under fluid flow compared to static culture using confocal microscopy, scanning electron microscopy (SEM), energy dispersive spectrometer (EDS), and transmission electron microscopy (TEM). Furthermore, a viability assay was used to assess cell's survival after exposing the treated cells to photothermal laser at different power densities and durations. We showed that when incubated with cancer cells, 2D MXene nanoparticles were successfully internalized into the cells resulting in increased intracellular temperatures when exposed to NIR laser. Interestingly, dynamic culture alone did not result in a significant increase in uptake suggesting the need for surface modifications for enhanced cellular uptake under shear stress.

Keywords: Cancer, photothermal therapy, static, dynamic, MXene

OPEN ACCESS

Edited by:
Arvind Chandrasekaran, North Carolina Agricultural and Technical State University, United States

Reviewed by:
Gurpreet Kaur, Panjab University, India
Geetha Manivasagam, VIT University, India

****Correspondence:***
Ahmed Elzatahry
aelzatahry@qu.edu.qa
Huseyin C. Yalcin
hyalcin@qu.edu.qa

Specialty section:
This article was submitted to Biomedical Nanotechnology, a section of the journal Frontiers in Nanotechnology

Received: *01 April 2021*
Accepted: *03 August 2021*
Published: *08 September 2021*

Citation:
Shurbaji S, Manaph NPA, Ltaief SM, Al-Shammari AR, Elzatahry A and Yalcin HC (2021) Characterization of MXene as a Cancer Photothermal Agent Under Physiological Conditions. Front. Nanotechnol. 3:689718. doi: 10.3389/fnano.2021.689718

INTRODUCTION

Cancer is a lethal widespread disease with no definitive treatment. Researchers have been working on cancer therapy for decades, with some improvements, yet many limitations persist (Guimarães et al., 2013). Malignant tumors are categorized into solid-localized tumors or metastatic tumors (Idikio, 2011). Localized tumors, like breast cancer, are mostly removed by surgery combined with chemotherapy or radiation therapy (Nounou et al., 2015). Although these are the most applied treatments, they are limited by the incomplete removal of the tumor by surgery which may lead to tumor recurrence (Tohme et al., 2017). Furthermore, chemotherapy and radiation therapy have many side effects such as damage to healthy tissue, hair loss, nausea, and bowel issues. To overcome these limitations, nanomaterials were extensively studied as a targeted drug delivery method for cancer therapy (Hussain, 2018). One of these materials is Ti_3C_2 also known as MXene, which is a 2D material where M stands for an early transition metal, X is carbon or nitrogen, and -ene is just like in

graphene which is the first 2D material discovered. MXene was studied for many biomedical applications including tumor detection (i.e., as contrast agents), cancer therapy, drug delivery, and antimicrobial effect (Lin et al., 2018). Additionally, MXene was shown to have a photothermal effect, which means that it can convert laser light energy to heat energy by surface plasmon resonance effect. Therefore, MXene was studied for cancer photothermal therapy by many researchers, who focused on killing cancer cells by heat leading to protein denaturation and eventual cell death (Liu et al., 2017; Liu et al., 2018). It was reported that MXene with a size around 180 nm can specifically reach the cancerous microenvironment by enhanced permeability and retention of EPR (Gazzi et al., 2019). However, to be most effective, photothermal agents need to bind to cancer cells and be internalized by these cells. Majority of photothermal studies on MXene for cancer treatment were conducted using cells in static culture. These studies did not consider the tumor biophysical microenvironment that is associated with fluid flow and shear stresses, which are important factors influencing cell/nanoparticle interactions including internalization (Xie, 2019; Shurbaji et al., 2020a). The oversimplified system in static culture might lead to misleading results, which in most cases contradict results obtained from *in vivo* animal experiments. This is because cells under fluid flow behave differently than in static culture due to the activation of flow responsive pathways that might influence their cellular adhesion and nanomaterial uptake (Ferlin et al., 2014; Ye et al., 2018). Photothermal therapy, which kills the cancer cells by heat (Jiang et al., 2020), might remove the tumor completely; hence, it is more superior compared to surgical removal. However, photothermal therapy can still induce side effects (damaging the nearby healthy tissues) if the material is not fully internalized by cancer cells (Sheng et al., 2017). Although MXene showed a good photothermal efficiency that makes it a potential candidate for photothermal therapy, the internalization of MXene into cancer cells was not studied extensively. Fluid flow in cell culture can influence the way that cells uptake the nanomaterials. Previous studies showed that fluid flow enhances material uptake compared to the static culture which may improve the therapeutic approach (Kang and Park, 2016).

Even though MXene is a relatively new material, it has been widely studied and modified for both *in vitro* and *in vivo* applications. However, the cellular internalization of MXene under different conditions has not been studied extensively. In this study, we investigated the photothermal efficiency of 2D MXene sheets by focusing on the influence of physiological fluid flows on the internalization of MXene into cancer cells.

MATERIALS AND METHODS

Chemicals

For MXene preparation, aluminum titanium carbide powder (Ti_3AlC_2 or MAX phase) was purchased from Carbon-Ukraine ltd. Hydrofluoric acid (HF, 48%) was supplied by Merck Schuchardt OHG, Germany. Dimethyl sulfoxide (DMSO) was obtained from Honeywell Riedel-de Haën®, Germany.

MXene Synthesis and Characterization

MXene was synthesized by following the protocol from Dr. Yury Gogotsi (Drexel University) who produced MXene for the first time (Alhabeb et al., 2017). In brief, 10 ml of 48% hydrofluoric acid was added to 1 g of Ti_3AlC_2 MAX phase with overnight stirring to allow for chemical etching of aluminum (Al) from Ti_3AlC_2 MAX phase. This was followed by water washes until a safe pH was achieved (pH = 5–6). After that, MXene was intercalated with DMSO and then delaminated using a probe sonicator with argon gas flowing, followed by 1-h centrifugation at 4°C.

The produced MXene sheets were characterized by X-Ray diffraction (XRD) to reveal the crystal structure using PAN analytical X-ray diffractometer. XRD was performed at 45 kV and 20 mA. The results were acquired from $2\theta = 5^{\circ}$ to 100°. Surface morphology and elemental analysis were assessed using NOVA NANOSEM 450 (N-SEM) and energy dispersive spectrometer (EDS), respectively. A voltage between 500 V and 30 kV was applied with a 10 mm distance between the sample and electron source, which is satisfactory to obtain good images. Talos transmission electron microscope (TEM) was used to further confirm the morphology of the produced MXene sheets. For image acquisition, the microscope was operated at 200 kV. A very thin layer of the sample was placed in a carbon-coated grid and then positioned on an electron beam produced by the electron gun. ZetaSIZER NANO-Malvern hosted at CAM was used to assess the surface charge of MXene. The device can find the zeta potential by using electrophoretic light scattering. MXene absorbance and the refractive index were collected from the literature of Berdiyorov (2016) and Li et al. (2017). MXene solution was diluted to 5 μg/ml before obtaining the measurements, and it was placed in a disposable folded capillary cell to be processed by the device.

To assess the light to the heat conversion efficiency of the produced nanosheets, FLIR C3 thermal camera was used to assess the temperature of MXene samples upon laser irradiation. MXene samples were exposed to laser at different power densities (PD = 1, 2, 3, and 5 W/cm^2) for 5 min.

Cell Culture

In this study, we used MDA-231 human breast cancer cells, from ATCC® (ATCC® HTB-26™). Cells were cultured in a complete media consisting of RPMI 1640 media (61870143-Thermofisher Scientific) supplemented with 10% fetal bovine serum (FBS) and 1% penicillin and streptomycin according to the supplier's protocol.

Static Cell Condition

Following the harvesting of 80% confluent cells in a T25 culture flask, they are washed twice in phosphate buffer saline (PBS) followed by trypsinization for 5 min using 0.25% trypsin. Then a complete cell media and antifungal solution were added to the trypsinized cells to stop the action of trypsin, which was followed by 5 min centrifugation at 1,000 rpm. Thereafter, the supernatant was removed, and 1 ml of complete media is added to the cell pellet and mixed thoroughly. A final density of 10,000 cells (375 cell/cm^2) in complete media was seeded in 40-mm-diameter

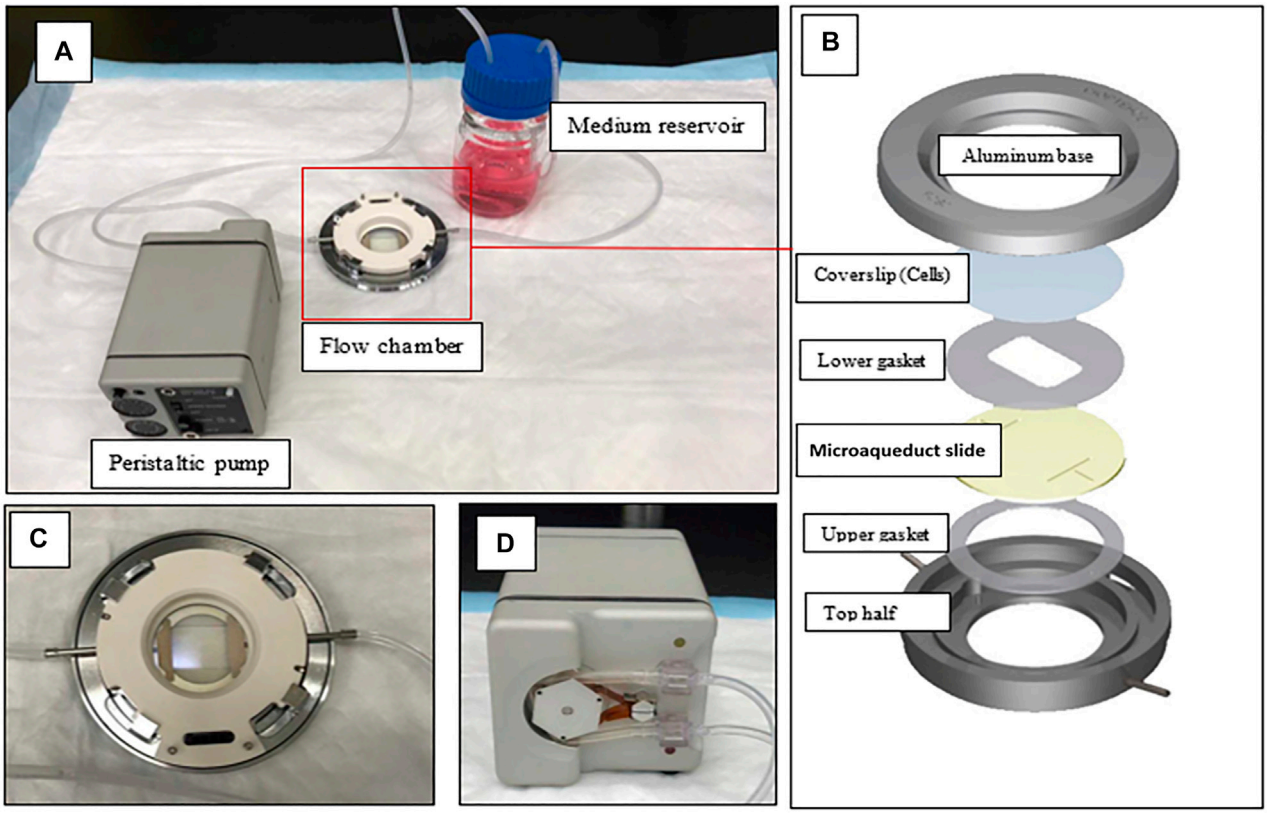

FIGURE 1 | Flow chamber setup. **(A)** The flow chamber is connected to the peristaltic pump from one side and the medium reservoir from the other side in a closed circuit. **(B)** Flow chamber assembly. **(C)** The flow chamber closer view **(D)** Back view of the peristaltic pump.

circular coverslips placed inside 50-mm-diameter Petri dishes, which were then incubated in a cell incubator at optimum conditions (37°C, 5% Co_2, and 95% air).

Dynamic Cell Condition

A parallel plate flow chamber (PPFC) was used to create dynamic conditions for cultured cells. Here, we used the FCS2 system from Bioptechs. A microperfusion peristaltic pump was used to generate flow over cultured cells. The flow rate was calculated using the HagenPoiseuille equation for a Newtonian fluid. A shear rate of 0.1 Dyn/cm^2 was used to model the interstitial flow fluid shear stress (FSS) over cultured cells. The flow of interstitial fluid was shown to induce FSS to the cancer cells within the localized tumor (Yao et al., 2012) with a shear rate of 0.1 (Dyn/cm^2) (Kang et al., 2016). After pump calibration and speed calculation, the pump was connected to Tygon tubing connecting the pump to the flow chamber in a closed circuit (**Figure 1**) (Shurbaji et al., 2020b). MXene was sonicated and then diluted in cell media to the desired concentration. 10,000 cells were seeded in a 40-mm-diameter circular coverslip which was then assembled in the chamber as in **Figure 1B**. After that, the whole setup was incubated in a cell incubator under optimum conditions for the desired incubation time (4 or 8 h). We tested two MXene concentrations of 100 and 200 μg/ml as based on previous work in our laboratory, 50 and below did not lead to internalization, and above 200 caused toxicity.

Exposure of Cells to Laser

VENUS series high stability benchtop laser was used to expose the cells to laser at a wavelength of 808 nm with different PDs (1, 3, or 5 W/cm^2) for different durations (5, 10, or 15 min).

Viability Assessment

After exposing the cells to MXene and laser, cell viability was assessed using an live/dead stain from ThermoFisher (Cat. No L3224), which includes calcein and ethidium homodimer-1. In brief, 5 μl calcein and 5 μl ethidium homodimer-1 were mixed with 10 ml serum-free media to make the stain at a final working concentration of 1 μM. The cells were incubated with the stain for 10 min at room temperature followed by fluorescent imaging using Olympus microscope IX73. Live images were taken by the GFP green filter, whereas dead images were taken by the C3Y red filter. Ten representative images were taken for live and dead cells at ×10 magnification. The images were then merged in ImageJ, and the live and dead cells were quantified to determine the viability percentage using the following formula:

Viability percentage = (Number of live cells)/(Total number of cells)×100%

Uptake Assessment

MXene uptake by cells was assessed by the following methods: Confocal microscopy, transmission electron microscopy (TEM), scanning electron microscopy (SEM), and energy dispersive spectrometer (EDS).

Confocal Microscopy

Zeiss confocal LSM microscope equipped with the ARIES imaging program was accessed from the laboratory in Weill Cornell Medical College in Qatar. The cells embedded on the slides were stained with the cytoplasmic marker (Calcein AM) and the nuclear marker (DAPI, D130 Thermofisher scientific). Then the cells were fixed in 4% paraformaldehyde for 15 min, washed twice in PBS, mounted, and coverslipped. The stained samples were visualized at ×63 magnification, and 2D and stacked images were obtained for the cytoplasm (Calcein AM, green channel), nucleus (DAPI, blue channel), and nanoparticles (phase-contrast). Images were analyzed using ImageJ software to produce 3D projections, 3D volumes, and sliced 3D volumes.

Transmission Electron Microscopy

The following protocol was used to prepare the samples for TEM imaging. Samples were fixed for one hour in a mixture of 2% paraformaldehyde and 2% glutaraldehyde (G5882-100, Sigma) followed by overnight fixation in 2% glutaraldehyde at 4°C. Samples were then washed twice in 0.1 M phosphate buffer and embedded in 2% agarose followed by 15 min centrifugation at 3,000 rpm to solidify. The agarose pellet was trimmed to <0.5 mm and post-fixed in 2% osmium tetroxide for one hour followed by 3–5 washes in distilled water. In contrast, samples were incubated in 2% uranyl acetate (22,400–4, EMS) for 30 min and then washed 3–5 times in distilled water. This was followed by serial dehydration in 30, 50, 70, and 90% acetone (for 15 min each) and three changes in 100% acetone (for 30 min each). For embedding, a medium formulation of Agar 100 resin (AGR1031, Agar Scientific) was prepared according to the manufacturer's protocol. Samples were gradually infiltrated in a 2:1 mix of acetone: resin, then in 1:1 mix and 1:2 mix of acetone: resin (for 30 min each) followed by overnight infiltration in 100% resin. This was then replaced with a fresh 100% resin for five hours infiltration before placing the samples in embedding molds that were filled carefully with a fresh 100% resin and cured in an oven at 60°C for 1–2 days. Ultra-thin sections (approximately 100 nm) were cut using ultra-microtome (Leica EM UC7), and sections were mounted on 200 mesh copper grids and coated in carbon before imaging in a transmission electron microscope (Talos F200C, ThermoFisher Scientific).

Scanning Electron Microscopy and Energy Dispersive Spectrometer

The cells embedded on slides were fixed with 2% glutaraldehyde for 24 h at 4°C. The slides were then washed twice in PBS followed by a series of dehydration steps in ethanol (50, 70, 80, 90, 95, and 100%) and allowed to air-dry. All slides were coated with gold (Au) to be conductive and allow for SEM and EDS analysis.

Cytoskeletal Staining

Changes in cytoskeletal structure have been shown in some studies to affect the cellular uptake of nanomaterials (Panariti et al., 2012). To reveal if the cytoskeletal structure is altered under fluid flow, cells were grown at 50% confluency and were either cultured in static or in dynamic conditions then fixed with 4% paraformaldehyde for 15 min. The samples were permeabilized using Triton X-100 solution, and then bovine serum albumin was added to block the unspecific bindings. The samples were then incubated overnight at 4°C with Alexa-488 actin labeled phalloidin antibody (A12379- Thermofisher scientific), which binds specifically to actin fibers in the cellular cytoskeleton. Following that, samples were mounted and coverslipped and were imaged using Olympus fluorescent microscope at ×60 magnification using the GFP filter.

Statistical Analysis

ANOVA test was performed to find statistical significance followed by the Tukey's test to compare the significance between the sample means ($n \geq 3$).

RESULTS

MXene Morphology and Characteristics

SEM images are represented in **Figure 2**. The MAX phase has a closely packed layered structure, which spread out after the removal of Al resembling an accordion (Tang et al., 2018) (**Figure 2B**). Delaminated single MXene sheets are represented in **Figure 2C**. Using SEM measurements, the average sheet size was found to be 190 ± 35 nm. The TEM image in **Figure 2B** further confirms the presence of 2D sheets as well as the sheet size. XRD was employed for the MAX phase, etched MAX, and MXene, and the results are represented in **Figure 2C**. Successful etching can be observed by the loss of Al peak from MAX pre-cursor at $2\theta \sim 39^{\circ}$ in both etched MAX and MXene. Comparing the MAX phase to etched MAX and MXene, it can be observed that the two peaks (002) and (004) become wider and less intense with a slight shift to lower angles. Diffraction peaks from $2\theta = 35^{\circ}$ to 45° were lost in MXene XRD which indicates delamination and loss of stacking. Furthermore, MXene surface charged was assessed and found to be −21.3 ± 0.643.

The thermal camera was used to assess the rise in MXene temperature after laser exposure. Here, MXene was dispersed in cell media and sonicated for 10 min at room temperature. After that, 100 ul of the solution was placed on a 96-well plate for laser exposure. Different laser power densities were applied for two MXene concentrations (100 and 200 ug/ml). For all the cases, it took the MXene one min to reach the maximum temperature which stays constant for the rest of the 5 min. After removing the incident laser light, it took ~4 min for the solution to reach 37°C.

The results in **Figure 3** show a trend, in which increasing the power densities in MXene concentrations results in increasing the temperature. However, similar temperature values were obtained for power densities of 3 and 5 W/cm^2,

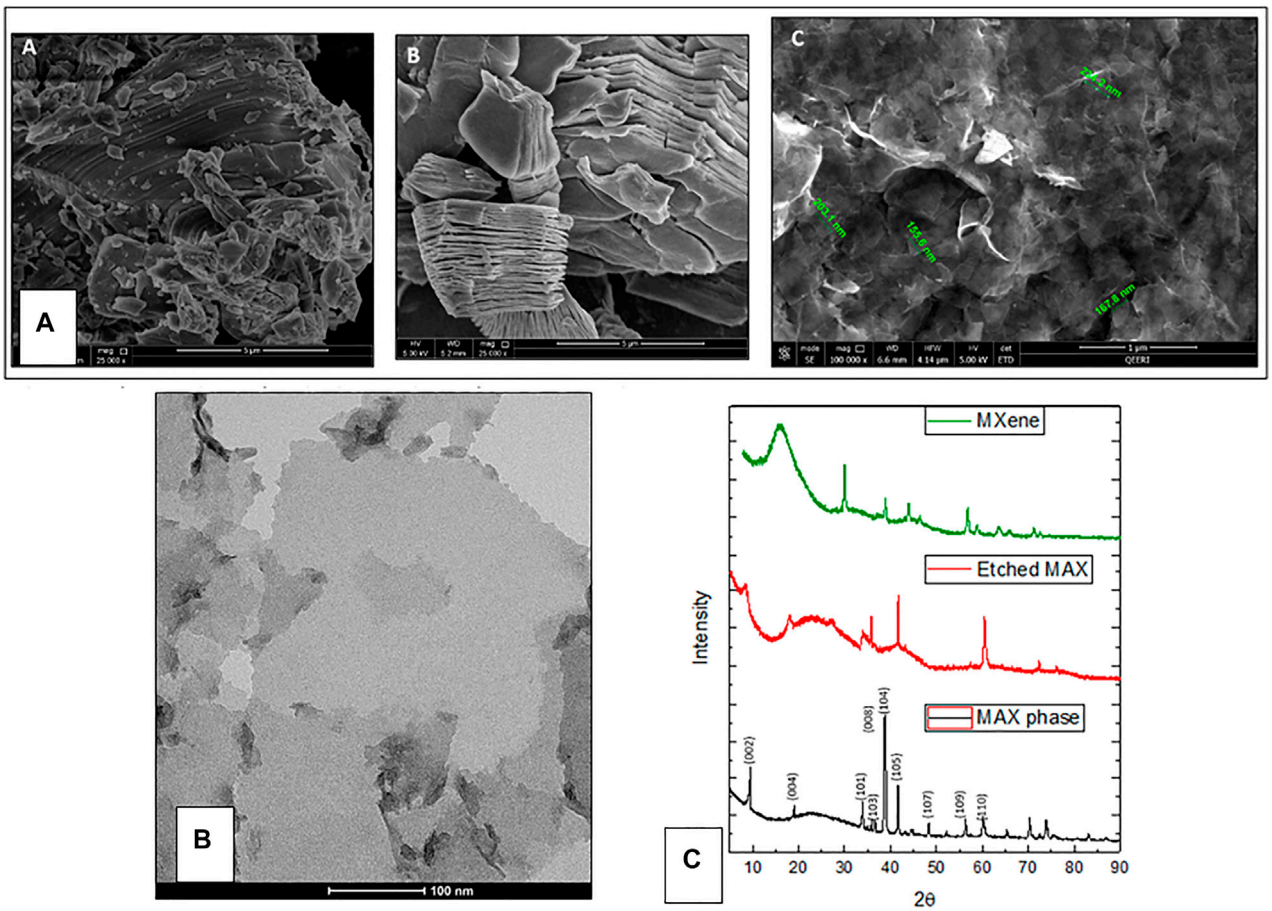

FIGURE 2 | (A) SEM images of MXene sheets. A) MAX phase, B) etched MAX phase, C) MXene nanosheets. **(B)** A representative TEM image showing a single MXene sheet. **(C)** XRD peaks for MAX phase, etched MAX, and MXene.

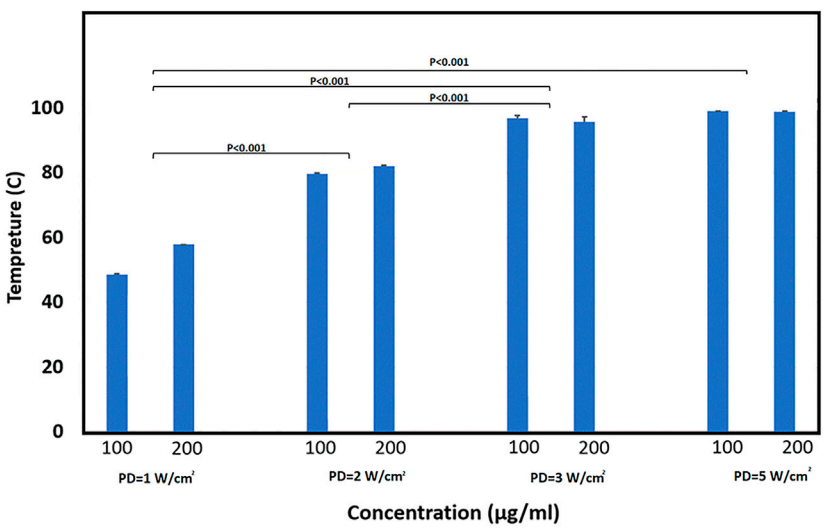

FIGURE 3 | Average temperature obtained when exposing cell media with different MXene concentrations (100 and 200 µg/ml) and exposed to different PDs (1, 2, 3, and 5 W/cm^2). Groups were analyzed by two-way ANOVA followed by a post hoc test. The *p*-value summery is < 0.001.

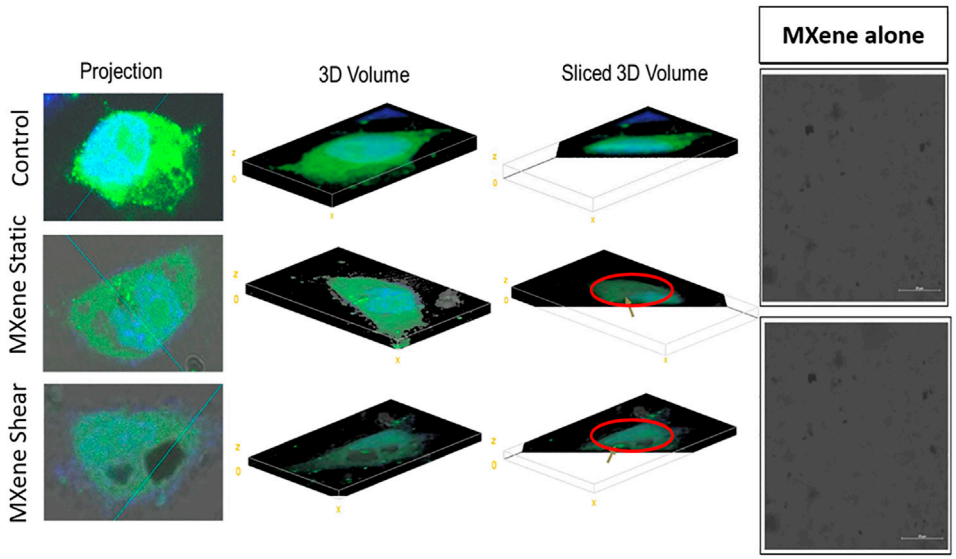

FIGURE 4 | Confocal images for MXene-treated cells under static and dynamic conditions. The golden arrow represents where MXene is located. The figure represents few MXene particles inside the cells (sliced 3D image) without any significant difference between static and dynamic conditions.

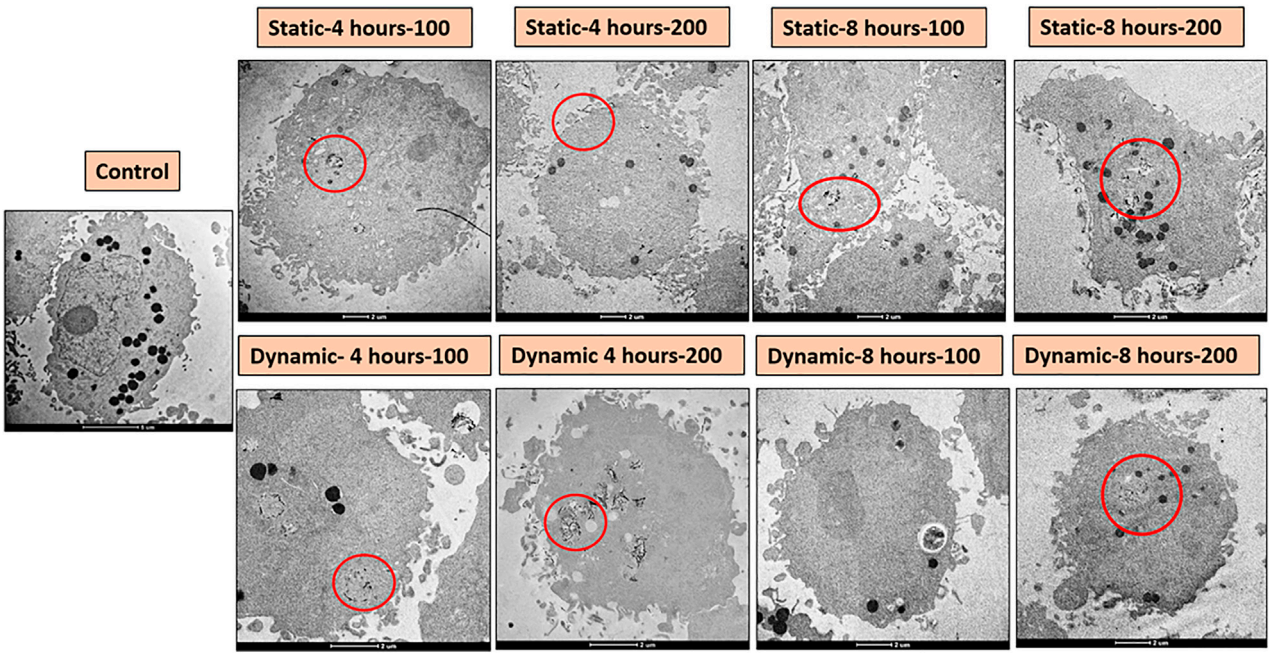

FIGURE 5 | TEM images for MDA-231 cells treated with MXene under different conditions. MXene 2D sheets are indicated by the red circles.

which might be because the temperature has reached the maximum value at ~99°C.

MXene Uptake by MDA-231 Cells Under Static and Dynamic Conditions

Confocal microscopy analysis was performed as a preliminary test to confirm that the material can be internalized by cancer cells, however MXene quantification was not possible as MXene was not fluorescently labeled. **Figure 4** represents MDA-231 cells treated with 100 µg/ml MXene under dynamic and static conditions for 4 h. The 3D crosssections show a few material uptakes without any difference between the two conditions.

To visualize the material clearly inside cancer cells, TEM was performed. **Figure 5** represents different TEM images for cells

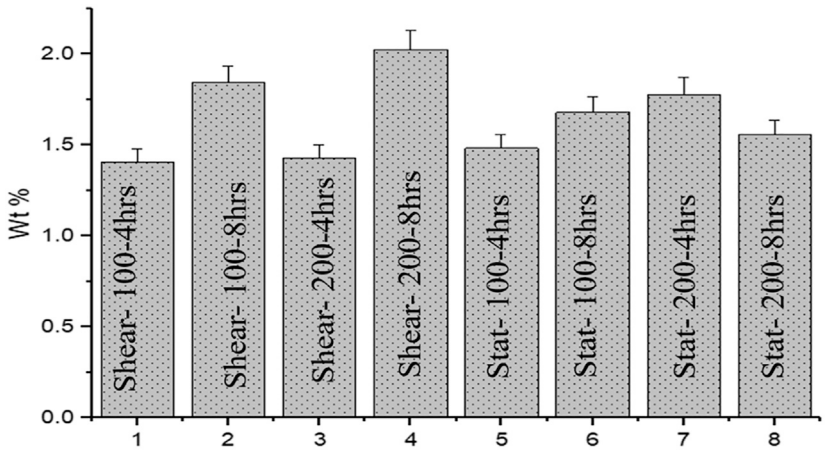

FIGURE 6 | Bar chart represents weight percentage (wt%) for Ti for 8 different cases. Different MXene concentrations and exposure durations did not show any significant difference in MXene uptake by MDA-231 cells.

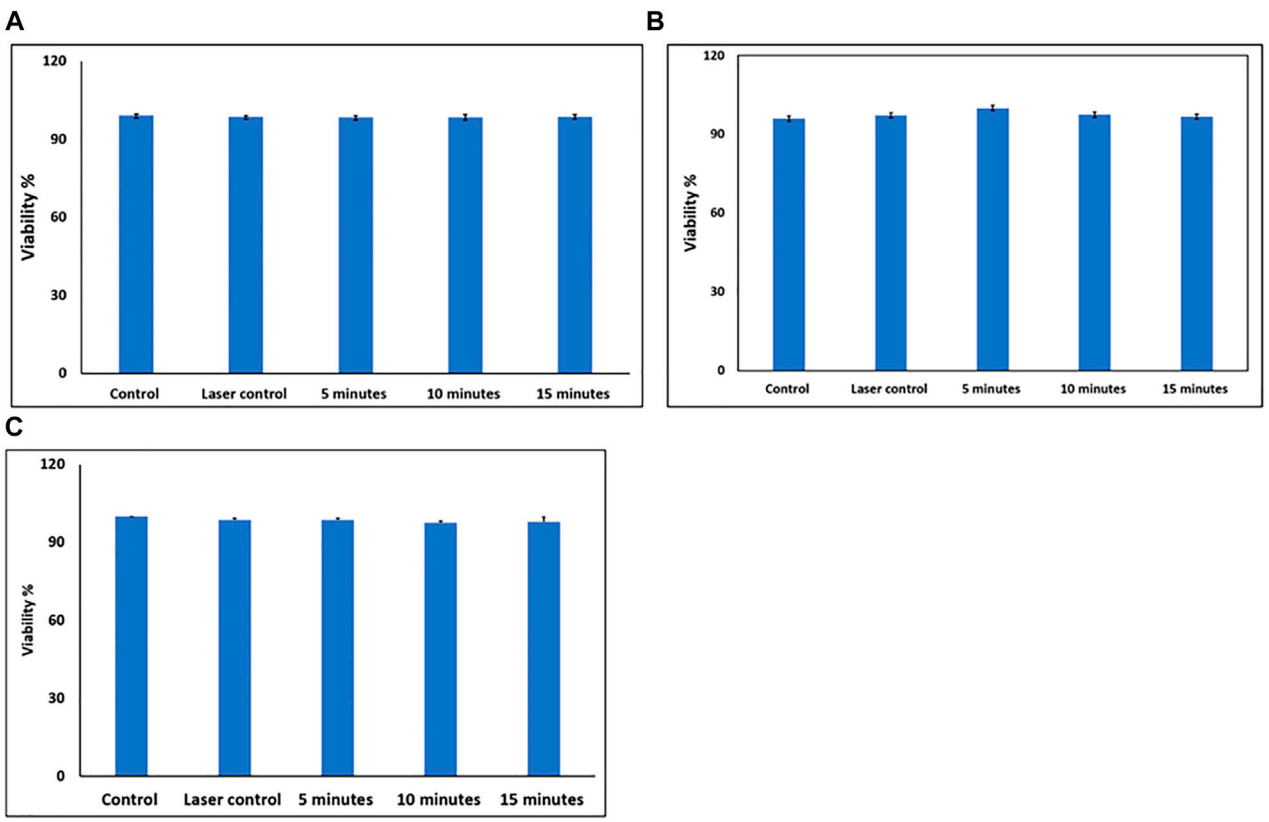

FIGURE 7 | (A) Cell viability after exposure to PD = 1 W/cm^2 for different durations (5, 10, and 15 min). **(B)** Cell viability after exposure to PD = 3 W/cm^2 for different durations (5, 10, and 15 min). **(C)** Cell viability after exposure to PD = 5 W/cm^2 for different durations (5, 10, and 15 min).

treated under different conditions. For the static and dynamic conditions, cells were treated with 100 or 200 μg/ml MXene and were exposed for four or 8 h. Material uptake was considered to occur if the material is attached to the cell's surface (association) or present inside the cell (internalization). As shown in **Figure 5**, few MXene particles were observed inside the cells in all conditions (indicated as red circle), and a slightly higher number of particles are presented when increasing the concentration. Nevertheless, the duration of exposure did not show any significant difference in MXene cellular uptake. Overall,

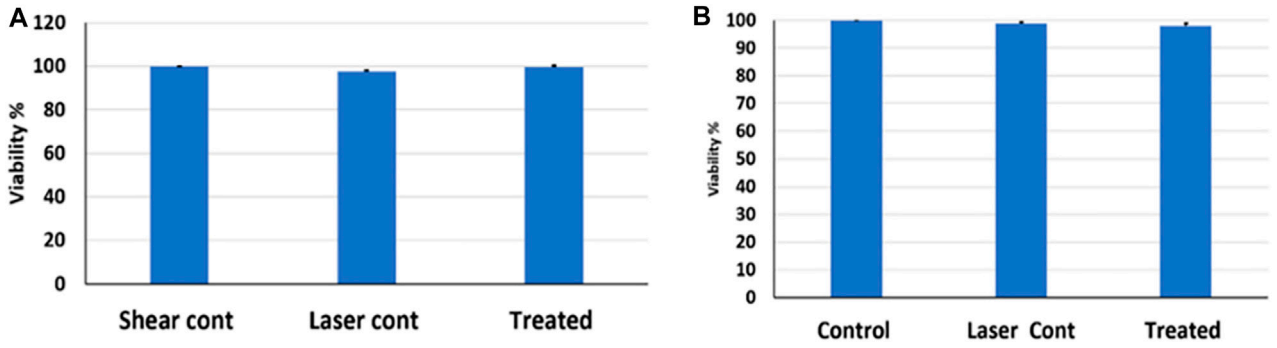

FIGURE 8 | (A) Cell viability after doubling the incubation time-laser exposure to PD = 5 W/cm^2 for 15 min, **(B)** Cell viability after doubling MXene concentration and laser exposure to PD = 5 W/cm^2 for 15 min.

the material uptake under all conditions is limited with only slight differences between all groups. **Figure 6** represents EDS results and shows the weight percentage of Ti inside MDA-231 cells in eight different conditions (as in TEM). The results show a non-significant difference between all groups. However, for the dynamic groups treated for 8 h duration, the uptake was slightly higher than the other groups, though the difference was not significant.

The Effect of Different Laser Power Densities and Exposure Times on Cell Viability

Cell viability after laser exposure was also assessed under different conditions to find out if the heat generated due to material internalization was sufficient to induce cell death. **Figure 7** shows bar charts for the viability of cells treated with 100 µg/ml MXene under fluid flow and then exposed to laser at different power densities (1, 3, and 5 W/cm^2) for different durations (5, 10, and 15 min). The viabilities for all the studied groups were similar to that of control groups, which indicates no significant effect of the applied power densities and durations on cells viability.

The Effect of Doubling the Incubation Time on Cell Viability

The incubation time might affect the material and cell interaction, as there will be more time for the particles to be internalized by the cells. Safi et al. showed that the cellular uptake of quantum dots was directly proportional to increasing the incubation time (Safi et al., 2016). To test that in our study, 200 µg/ml MXene was incubated with the cells under fluid flow for 8 h (doubling the incubation time) and then exposed to laser at PD = 5 for 15 min. **Figure 8A** shows no difference in cell viability in control groups compared to the treated groups.

The Effect of Doubling MXene Concentration on Cell Viability

The concentration of nanomaterials plays a role in material uptake by cells, i.e., changing the concentration will influence the way that the cells uptake the materials. As the concentration increases, there is a higher tendency that the material will form aggregates. These aggregates may affect the size of the material; thus, the uptake route might be altered (Mustafa, 2011). **Figure 8B** represents a bar chart for cells treated with 200 µg/ml MXene for 4 h and then exposed to laser at PD = 5 for 15 min. The results indicate that doubling the concentration of MXene did not affect cell viability, i.e., no cell death was induced.

Effect of Shear Stress on Cell's Cytoskeleton

In this study, we are examining the MXene uptake by cancer cells under dynamic culture and static culture. Previous studies reported that fluid flow can increase particle uptake due to the formation of cytoskeletal stress fibers and membrane ruffles (Ispanixtlahuatl-meráz et al., 2017). To examine if cells under dynamic conditions would have stress fibers, we stained actin cytoskeletal for the cells under static and dynamic conditions. Consistent with previous studies, the stress fibers for the cells exposed to flow were clear. Interestingly, MXene uptake showed no difference under fluid flow in our experiments (**Figure 9**).

Determination of Internalized MXene Concentration

In an attempt to quantify the concentration of internalized MXene, we first cultured cells with 200 µg/ml MXene for 4 h under static conditions, then exposed them to a photothermal laser for 15 min, and measured the temperature of cells with the thermal camera. Cell temperature for PD 1 W/cm^2 was 33.9°C, for PD 3 W/cm^2 was 38.7°C, and for PD 5 W/cm^2 was 42.8°C. To identify what concentrations of MXene these temperatures are matching, we exposed different concentrations of MXene alone at different PDs and match those with temperature results obtained from culture experiments. Using the thermal camera, we tried to find the maximum temperature that can be achieved when treating the cells with 200 µg/ml MXene for 15 min at different power densities. The MXene concentration that gives approximately the same temperatures for MXene/cell culture and

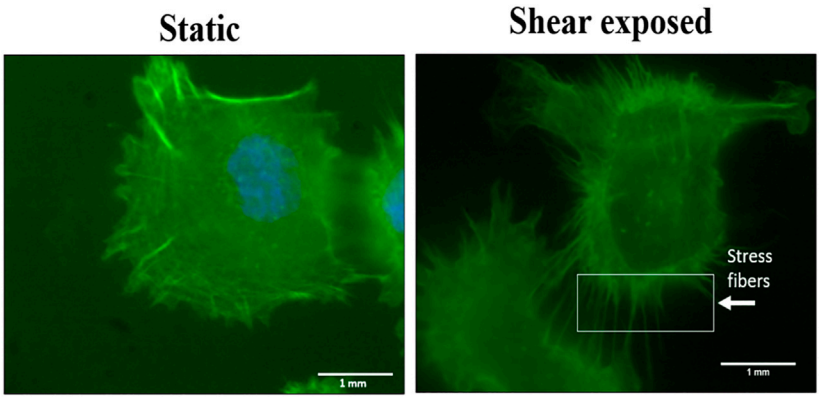

FIGURE 9 | Cytoskeletal staining for MDA-231 cells under static and fluid flow conditions. Actin filaments stress fibers formation after being exposed to shear stress at a low shear rate for 8 h.

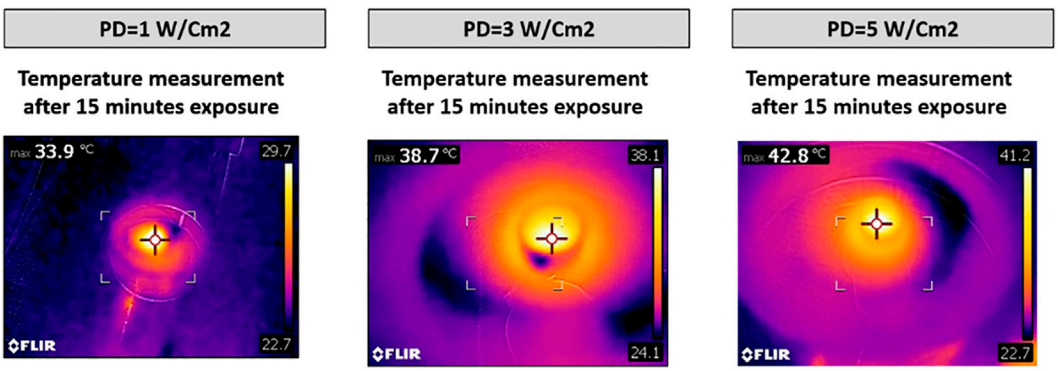

FIGURE 10 | Temperature measurement for cells treated with 200 μg/ml MXene then exposed to laser at different PDs for 15 min.

MXene alone measurements was 3 μg/ml, suggesting internalized MXene concentration is about 3 μg/ml (**Figures 10**, **11**).

DISCUSSION

MXene has been introduced as a new nanomaterial recently and has been studied since then for many biomedical applications including cancer photothermal therapy. In this study, we examined different factors influencing the internalization of MXene for cancer cells to be used as a photothermal agent. Upon successful production of MXene following the guidelines from Dr. Yury's laboratory where MXene was first produced (Alhabeb et al., 2017) (Hussein et al., 2019), breast cancer cells were cultured at different concentrations of MXene. The experiments were repeated for static and physiologically relevant dynamic conditions. A variety of imaging and structural analysis techniques were adapted to qualitatively and quantitatively assess MXene internalization. To assess the photothermal efficiency of internalized MXene, after the completion of culture with MXene, cell cultures were exposed to the photothermal laser. Cell viability and cell temperatures were measured following laser exposures.

According to our results, produced MXenes had desired structural characteristics. XRD results showed a good etching due to the loss of Al peak from MAX precursor at $2\theta \sim 39^{\circ}$ in both etched MAX and MXene. Comparing the MAX phase to etched MAX and MXene, it can be observed that the two peaks (002) and (004) become wider and less intense with a slight shift to lower angles. Diffraction peaks from $2\theta = 35^{\circ}$ to 45° were lost in MXene XRD which indicates delamination and loss of stacking. All of these observations were similar to MXene XRD patterns from the literature Naguib (2011). MXene size was around 190 nm ± 35 which has been confirmed by two methods (SEM and TEM) and which has been reported to be optimum for biomedical applications, especially for photothermal therapy (Lin et al., 2017).

In the study, we cultured cells under different MXene concentrations for a variety of different durations. Also, the effect of fluid flow in particle internalization was assessed by culturing under static and dynamic conditions. Interestingly, particle concentration, culture duration as well as culture type

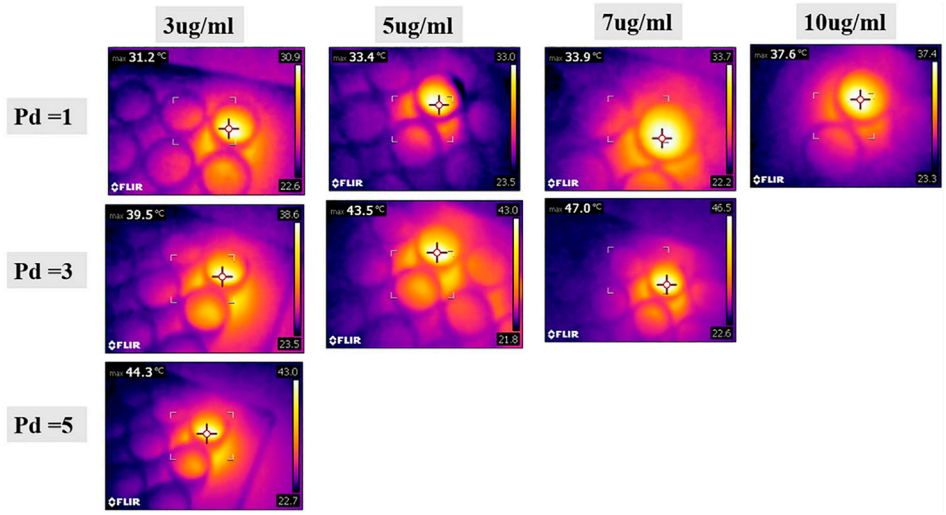

FIGURE 11 | Temperature measurements obtained when MXene with different dilutions (diluted with PBS) is exposed to laser with different PDs. These measurements were matched with temperature measurement obtained when the cells are treated with MXene, to approximately assess the concentration of MXene internalized by the cells (3 μg/ml).

did not influence cellular uptake. Although stress fibers were formed after exposure to shear stress, cellular uptake was not different in shear exposed cells compared to static culture. This suggests that the uptake, in this case, is not cell or shear stress-related, but particle-related. The material uptake was not influenced by shear stress probably due to the negatively charged surface and due to the presence of negative ions as functional groups (-OH group, fluorine, and oxygen) (Jing Zhang and Li, 2018; Tian et al., 2019). Since both cell surface and MXene are negatively charged, these charge similarities will prevent a good electrostatic interaction between cells and MXene, leading to low cellular association and uptake (Jing Zhang and Li, 2018). Moreover, MXene was not functionalized or coated with specific ligands that can bind to specific receptors on the cell's surface. This could have led to lower uptake as well as non-homogenous internalization in our study.

In addition to that, Mxene has a 2D shape, which might affect internalization. Some studies suggested better uptake of spherical nanoparticles compared to rod-shaped or 2D nanomaterials (Tian et al., 2019). These studies suggested that the cell membrane wrapping and internalization of rod-shaped materials are not desirable. The morphology of nano-materials can affect their cellular uptake. This relation was speculated to the area on the cell membrane covered by the particle. As in rod-shaped or 2D material, more area in cell surface would be covered compared to spherical nanoparticles which will block some of the existing surface receptors leading to fewer particle interactions and less uptake (Murugan et al., 2015).

MXene alone showed a good light to heat conversion efficiency, which was positively correlated with increased PD. However, PD at 3 and 5 W/cm^2 did not show a significant difference which could mean there is a maximum limit for heating MXene, and beyond this limit (~99°C), there will be no further increase in temperature even when increasing the MXene concentration. That is, all MXene 2D sheets were light-activated. However, our results for cells treated with MXene indicated there was a limit for the uptake of the particles, and no further uptake beyond that limit would be possible. Particularly, there was no temperature increase beyond 44°C in all conditions, and this was not sufficient to cause protein denaturation and induce cell death (Xie, 2011). Additionally, wt% of Ti was the same in all the cases. Therefore, we concluded that a maximum of 3 μg/ml MXene could be internalized by the cells in our experiments, however this was not sufficient for the photothermal therapy to kill the cells.

For better Mxene/cell interaction, we aim to modify the MXene surface. Rather than passive targeting, we are now changing the surface charge of MXene by coating it with biocompatible material like polyethylene glycol (PEG). As it was reported by Zhang et al. that polyethylene glycol-modified cobalt carbide nanoparticles (Co2C-PEG NPS) which is another type of MXene, showed a good PTT efficiency both *in vitro* and *in vivo*, titanium has a good light to heat conversion efficiency; however, since internalization was hindered, we can try PEG modification as reported by Zhang et al. (2020). However, we expect changes in the size of MXene after coating (it will become larger) which might influence the uptake. For that, other approaches like producing MXene quantum dots or adding cancer-specific ligands are into considerations (Shurbaji et al., 2020a). A great approach was reported by Zhou (2020) where they used Nb_2C MXene/zein bio-injection for better targeting of the MXene at the tumor site as zein can trap the MXene and improve the ablation efficiency. In their study, they reported a complete eradication of 4T1 breast cancer cells. An additional

approach for material targeting, reported by Liu et al., their study is based on chemo-photothermal therapy, where they produced the heterostructure titanium carbide-cobalt nanowires (Ti_3C_2-CoNWs) nanocarrier for controlled delivery and release of the anticancer drug doxorubicin. They reported that the synergistic chemo-photothermal therapeutic effect exhibits a strong killing ability for cancer cells than that of chemotherapy or PTT alone (Liu, 2020). One of the great advantages of MXene sheets is that its surface can be incorporated with nanoparticles, and there are many regrading nanoparticles with good plasmon resonance, one of these is Cu_5FeS_4 which was reported by Yuan et al. (2020) to have a good heat conversion efficiency which can reach up to 50%.

CONCLUSION

In this work, MXene 2D material was prepared for potential use in photothermal therapy in cancer. Both cellular viability and uptake were determined for MXene and the laser exposed cells. Cancer cells under fluid flow were exposed to MXene at different concentrations (100 μg/ml and 200 μg/ml) and durations (4 and 8 h) as well as to different laser power densities (1, 3, and 5 W/cm^2) and durations (5, 10, and 15 min). None of these conditions showed cell death after MXene treatment and laser exposure, which might be because the increase in temperature was not sufficient to induce cellular damage. When MXene cellular uptake was assessed, we found few particles were uptaken with non-homogenous distribution, in which some cells could fully internalize the MXene while other cells showed surface association only. Moreover, no difference in cellular uptake was noticed between static and dynamic culture. This suggests that the cells are unable to uptake the material, probably due to its negatively charged surface that does not form a good electrostatic interaction with the cell's surface that is also negatively charged.

Generally, MXene can be a good candidate for photothermal therapy for cancer treatment, but its cellular internalization should be enhanced. This can be achieved by coating the MXene surface with certain ligands that are specific to cancer cells.

DATA AVAILABILITY STATEMENT

The original contributions presented in the study are included in the article/**Supplementary Material**, further inquiries can be directed to the corresponding authors.

AUTHOR CONTRIBUTIONS

SS: Experimental planning-Conduction of experiments-original draft writing. NM : TEM experimental planning, troubleshooting, analysis, and draft revision. SL: TEM experimental planning, troubleshooting, analysis, and draft revision. AE: TEM experimental planning, troubleshooting, analysis, and draft revision. AE: conceptualization and supervision. HY: conceptualization, experimental planning, supervision, and final approval for the manuscript publication.

FUNDING

This work was supported by Qatar University internal grant (QUST-1-CAS-2019-37). The publication of this article was funded by the Qatar National Library.

ACKNOWLEDGMENTS

We would like to acknowledge the contribution of Core Labs and its personnel in Qatar Environment & Energy Research Institute for performing ultra-microtome sectioning and TEM imaging used in this study. We would like also to thank Isra Marei (Cornell medical labs) for performing the confocal imaging used in this study.

SUPPLEMENTARY MATERIAL

The Supplementary Material for this article can be found online at: https://www.frontiersin.org/articles/10.3389/fnano.2021.689718/full#supplementary-material

REFERENCES

Alhabeb, M., Maleski, K., Anasori, B., Lelyukh, P., Clark, L., and Sin, S. (2017). Guidelines for Synthesis and Processing of Two-Dimensional Titanium Carbide ($Ti_3C_2T_x$ MXene). *Chem. Mater.* 18, 7633–7644. doi:10.1021/acs.chemmater.7b02847

Berdiyorov, G. R. (2016). Optical Properties of Functionalized Ti3C2T2 (T = F, O, OH) MXene: First-Principles Calculations. *AIP Adv.* 6 (5). doi:10.1063/1.4948799

Ferlin, K. M., Prendergast, M. E., Miller, M. L., Nguyen, B. N. B., Kaplan, D. S., and Fisher, J. P. (2014). Development of a Dynamic Stem Cell Culture Platform for Mesenchymal Stem Cell Adhesion and Evaluation. *Mol. Pharm.* 11 (7), 2172–2181. doi:10.1021/mp500062n

Gazzi, A., Fusco, L., Khan, A., Bedognetti, D., Zavan, B., Vitale, F., et al. (2019). Photodynamic Therapy Based on Graphene and MXene in Cancer Theranostics. *Front. Bioeng. Biotechnol.* 7. doi:10.3389/fbioe.2019.00295

Guimarães, S., Herlinger, A. L., Madeira, K. P., Teixeira, S. F., and Amorim, G. M. (2013). "Conventional Cancer Treatment," in *Cancer Treatment - Conventional and Innovative Approaches*, 2–36.

Hussain, S. (2018). Utility of Nanomedicine for Cancer Treatment. *J. Nanomed. Nanotechnol.* 09 (01), 1–6. doi:10.4172/2157-7439.1000481

Hussein, E. A., Zagho, M. M., Rizeq, B. R., Younes, N. N., Pintus, G., Mahmoud, K. A., et al. (2019). Plasmonic MXene-Based Nanocomposites Exhibiting Photothermal Therapeutic Effects with Lower Acute Toxicity Than Pure MXene. *Int. J. Nanomedicine* 14, 4529–4539. doi:10.2147/IJN.S202208

Idikio, H. A. (2011). Human Cancer Classification: A Systems Biology- Based Model Integrating Morphology, Cancer Stem Cells, Proteomics, and Genomics. *J. Cancer* 2 (1), 107–115. doi:10.7150/jca.2.107

Ispanixtlahuatl-meráz, O., Schins, R. P. F., and Chirino, Y. I. (2017). Environmental Science Nano Cell Type Specific Cytoskeleton Disruption Induced by Engineered Nanoparticles. *Environ. Sci. Nano*. doi:10.1039/C7EN00704C

Jiang, J., Che, X., Qian, Y., Wang, L., Zhang, Y., and Wang, Z. (2020). Bismuth Sulfide Nanorods as Efficient Photothermal Theragnosis Agents for Cancer Treatment. *Front. Mater.* 7, 1–11. doi:10.3389/fmats.2020.00234

Kang, T., Park, C., Choi, J. S., Cui, J. H., and Lee, B. J. (2016). Effects of Shear Stress on the Cellular Distribution of Polystyrene Nanoparticles in a Biomimetic Microfluidic System. *J. Drug Deliv. Sci. Technol.* 31, 130–136. doi:10.1016/j.jddst.2015.12.001

Kang, T., and Park, C. (2016). Investigation of Biomimetic Shear Stress on Cellular Uptake and Mechanism of Polystyrene Nanoparticles in Various Cancer Cell Lines. *Arch. Pharm. Res.* 39 (12), 1663–1670. doi:10.1007/s12272-016-0847-0

Li, R., Zhang, L., Shi, L., and Wang, P. (2017). MXene Ti 3 C 2 : An E Ff Ective 2D Light-To-Heat Conversion Material. *ACS Nano* 4, 3752–3759. doi:10.1021/acsnano.6b08415

Lin, H., Chen, Y., and Shi, J. (2018). "Insights into 2D MXenes for Versatile Biomedical Applications: Current Advances and Challenges Ahead. *Adv. Sci.* 1800518. doi:10.1002/advs.201800518

Lin, H., Gao, S., Dai, C., Chen, Y., and Shi, J. (2017). *"A Two-Dimensional Biodegradable Niobium Carbide (MXene) for Photothermal Tumor Eradication in NIR - I and NIR-II Biowindows*, 16235–16247. doi:10.1021/jacs.7b07818

Liu, G., Zou, J., Tang, Q., Yang, X., and Zhang, Y. (2017). Surface Modified Ti3C2 MXene Nanosheets for Tumor Targeting Photothermal/Photodynamic/Chemo Synergistic Therapy Surface Modified Ti 3 C 2 MXene Nanosheets for Tumor Targeting Photothermal/Photodynamic/Chemo Synergistic Therapy. *ASC Appl. Mater. Interfaces* 9, 40077–40086. doi:10.1021/acsami.7b13421

Liu, Y. (2020). Two-dimensional MXene/cobalt Nanowire Heterojunction for Controlled Drug Delivery and Chemo-Photothermal Therapy. *Mater. Sci. Eng. C*, 116, 111212. doi:10.1016/j.msec.2020.111212

Liu, Z., Lin, H., Zhao, M., Dai, C., Zhang, S., Peng, W., et al. (2018). 2D Superparamagnetic Tantalum Carbide Composite MXenes for Efficient Breast-Cancer Theranostics. *Theranostics* 8–6. doi:10.7150/thno.23369

Murugan, K., Choonara, Y. E., Kumar, P., Bijukumar, D., du Toit, L. C., and Pillay, V. (2015). Parameters and Characteristics Governing Cellular Internalization and Trans-barrier Trafficking of Nanostructures. *Int. J. Nanomedicine*, 2191–2206. doi:10.2147/IJN.S75615

Mustafa, T. (2011). Impact of Gold Nanoparticle Concentration on Their Cellular Uptake by MC3T3-E1 Mouse Osteoblastic Cells as Analyzed by Transmission Electron Microscopy Nanomedicine & Nanotechnology. *J. Nanomdeicine Nanotechnol.* 2 (6). doi:10.4172/2157-7439.1000118

Naguib, M. (2011). Two-Dimensional Nanocrystals Produced by Exfoliation of Ti 3 AlC 2. *Adv. Mater.*, 4248–4253. doi:10.1002/adma.201102306

Nounou, M. I., Elamrawy, F., Ahmed, N., Abdelraouf, K., Goda, S., and Syed-Sha-Qhattal, H. (2015). Breast Cancer: Conventional Diagnosis and Treatment Modalities and Recent Patents and Technologies. *Breast Cancer(Auckl)* 9s2, S29420–S29434. doi:10.4137/BCBCR.S29420

Panariti, A., Miserocchi, G., and Rivolta, I. (2012). The Effect of Nanoparticle Uptake on Cellular Behavior: Disrupting or Enabling Functions? *Nanotechnol. Sci. Appl.* 5 (1), 87–100. doi:10.2147/NSA.S25515

Safi, M., Domitrovic, T., Kapur, A., Aldeek, F., Johnson, J. E., and Mattoussi, H. (2016). Intracellular Delivery of Luminescent Quantum Dots Mediated by a Virus-Derived Lytic Peptide Intracellular Delivery of Luminescent Quantum Dots Mediated by a Virus- Derived Lytic Peptide * Correspondence Author. *BC Bioconjugate Chem.* doi:10.1021/acs.bioconjchem.6b00609

Sheng, W., Seare, W. J., and Almutairi, A. (2017). "Review of the Progress toward Achieving Heat Confinement — the Holy Grail of Photothermal Therapy Confinement — the Holy Grail of Photothermal Therapy. *J. Biomed. Opt.* 22 (8). doi:10.1117/1.JBO.22.8.080901

Jing Zhang, Y. Z., and Li, S. (2018). Chemical Stability of Ti 3 C 2 MXene with Al in the Temperture Range 500-700C, *Materials (Basel)*, 1–9. doi:10.3390/ma11101979

Shurbaji, S., Al-Ruweidi, M. K. A. A., Ali, F. H., Benslimane, F. M., and Yalcin, H. C. (2020). Application of a Flow-Induced Stress Wave and Investigation of Associated Injuries on Cell Monolayers Using a Parallel Plate Flow Chamber. *Methods Protoc.* 3 (4), 1–9. doi:10.3390/mps3040065

Shurbaji, S., Anlar, G. G., Hussein, E. A., Elzatahry, A., and Yalcin, H. C. (2020). Effect of Flow-Induced Shear Stress in Nanomaterial Uptake by Cells: Focus on Targeted Anti-cancer Therapy. *Cancers (Basel)* 12 (7), 1–16. doi:10.3390/cancers12071916

Tang, Y., Yang, C., and Que, W. (2018). A Novel Two-Dimensional Accordion-like Titanium Carbide (MXene) for Adsorption of Cr(VI) from Aqueous Solution. *J. Adv. Dielectr.* 8 (5). doi:10.1142/S2010135X18500352

Tian, W., Vahidmohammadi, A., and Hamedi, M. M. (2019). Layer-by-layer Self-Assembly of Pillared Two-Dimensional Multilayers. *Nat. Commun.*, 1–10. doi:10.1038/s41467-019-10631-0

Tohme, S., Simmons, R. L., and Tsung, A. (2017). Surgery for Cancer: A Trigger for Metastases. *Cancer Res.* 77 (7), 1548–1552. doi:10.1158/0008-5472.CAN-16-1536

Xie, X. (2011). Effect of Hyperthermia on Invasion Ability and TGF-SS 1 Expression of Breast Carcinoma MCF-7 Cells. *Oncol. Rep.* 10, 1573–1579. doi:10.3892/or.2011.1240

Xie, Z. (2019). Biocompatible Two-Dimensional Titanium Nanosheets for Multimodal Imaging-Guided Cancer Theranostics. *ACS Appl. Mater. Inter.* 11, 22129–22140. doi:10.1021/acsami.9b04628

Yao, W., Li, Y., and Ding, G. (2012). "Interstitial Fluid Flow: The Mechanical Environment of Cells and Foundation of Meridians," *Evidence-Based Complement. Altern. Med.*, 2012. doi:10.1155/2012/853516

Ye, H., Shen, Z., Yu, L., Wei, M., and Li, Y. (2018). Manipulating Nanoparticle Transport within Blood Flow through External Forces: An Exemplar of Mechanics in Nanomedicine. *Proc. R. Soc. A. Math. Phys. Eng. Sci.* 474, 2211. doi:10.1098/rspa.2017.0845

Yuan, L., Hu, W., Zhang, H., Chen, L., Wang, J., and Wang, Q. (2020). Cu5FeS4 Nanoparticles with Tunable Plasmon Resonances for Efficient Photothermal Therapy of Cancers. *Front. Bioeng. Biotechnol.* 8, 1–10. doi:10.3389/fbioe.2020.00021

Zhang, D-Y., Xu, H., He, T., Younis, M. R., Zeng, L., Liu, H., et al. (2020). Cobalt Carbide-Based Theranostic Agents for *In Vivo* Multimodal Imaging Guided Photothermal Therapy. *Nanoscale* 12 (13). doi:10.1039/D0NR00468E

Zhou, B. (2020). *In Situ* phase-changeable 2D MXene/zein Bio-Injection for Shear Wave Elastography-Guided Tumor Ablation in NIR-II Bio-Window. *J. Mater. Chem. B* 8 (24), 5257–5266. doi:10.1039/d0tb00519c

Conflict of Interest: The authors declare that the research was conducted in the absence of any commercial or financial relationships that could be construed as a potential conflict of interest.

Publisher's Note: All claims expressed in this article are solely those of the authors and do not necessarily represent those of their affiliated organizations, or those of the publisher, the editors, and the reviewers. Any product that may be evaluated in this article, or claim that may be made by its manufacturer, is not guaranteed or endorsed by the publisher.